WILEY-VCH

ADVANCED HEALTHCARE MATERIALS

Supporting Information

for *Adv. Healthcare Mater.*, DOI: 10.1002/adhm.202100021

Rapid characterization and quantification of extracellular vesicles by fluorescence-based microfluidic diffusion sizing

*Carolina Paganini, Britta Hettich, Marie R.G. Kopp, Adam Eördögh, Umberto Capasso Palmiero, Giorgia Adamo, Nicolas Touzet, Mauro Manno, Antonella Bongiovanni, Pablo Rivera-Fuentes, Jean-Christophe Leroux, Paolo Arosio**

Supporting Information

Rapid characterization and quantification of extracellular vesicles by fluorescence-based microfluidic diffusion sizing

Carolina Paganini, Britta Hettich, Marie R.G. Kopp, Adam Eördögh, Umberto Capasso Palmiero, Giorgia Adamo, Nicolas Touzet, Mauro Manno, Antonella Bongiovanni, Pablo Rivera-Fuentes, Jean-Christophe Leroux, Paolo Arosio*

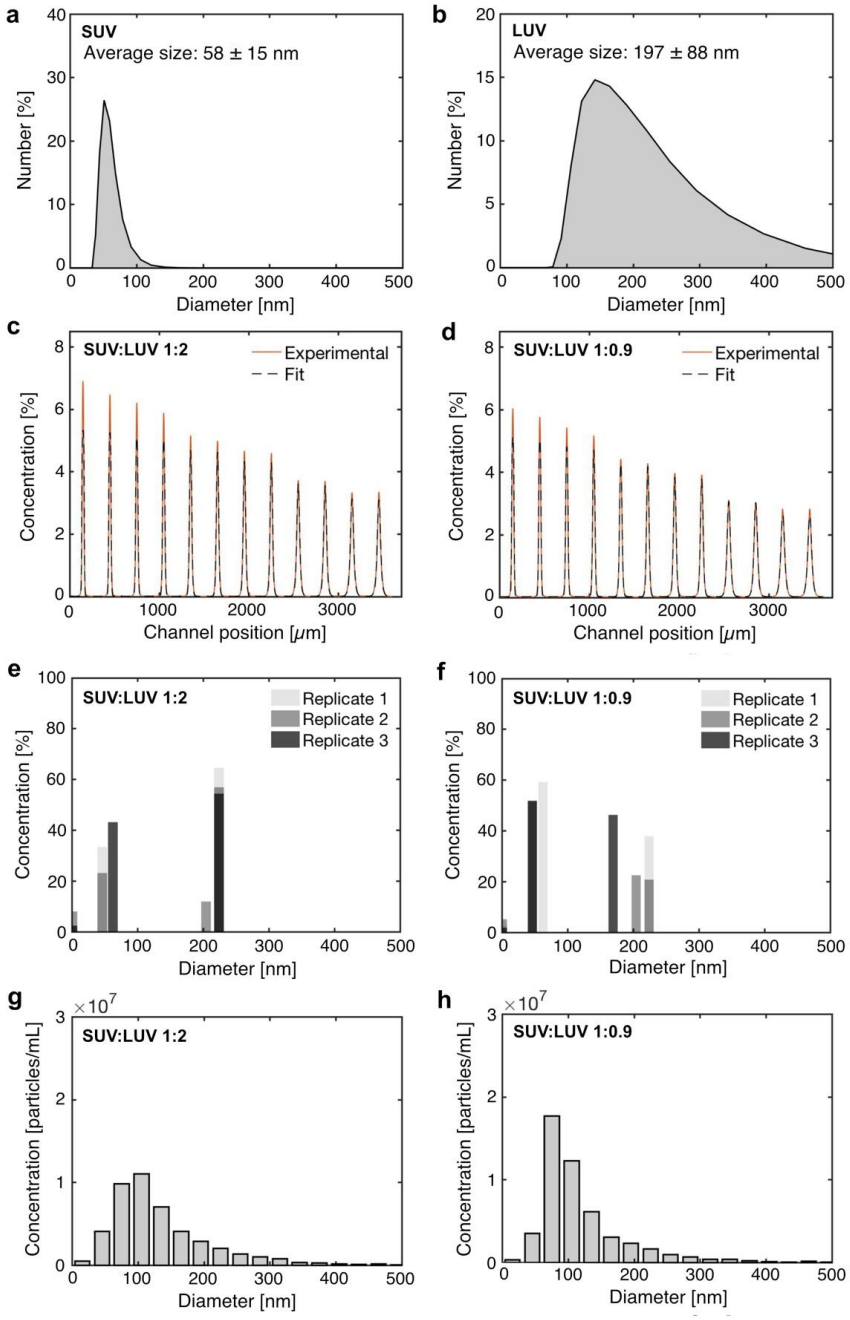

Figure S1. Characterization of SUVs and LUVs mixtures by fluoMDS and NTA. (a,b) The size distributions of the SUV and LUV samples were measured by DLS. (c,d) Mixtures of SUV and LUV were analyzed by fluoMDS by measuring the diffusion profiles of the sample at 12 positions in the microfluidic channel (red line) and fitting them with a linear combination of simulated profiles from a library of standards (black dashed line). (e,f) The distributions of the diffusion coefficients obtained from the fitting for the mixtures of SUV and LUV were translated into the size distributions of the samples. (g,h) The mixtures of SUV and LUV were also sized by NTA in light scattering mode.

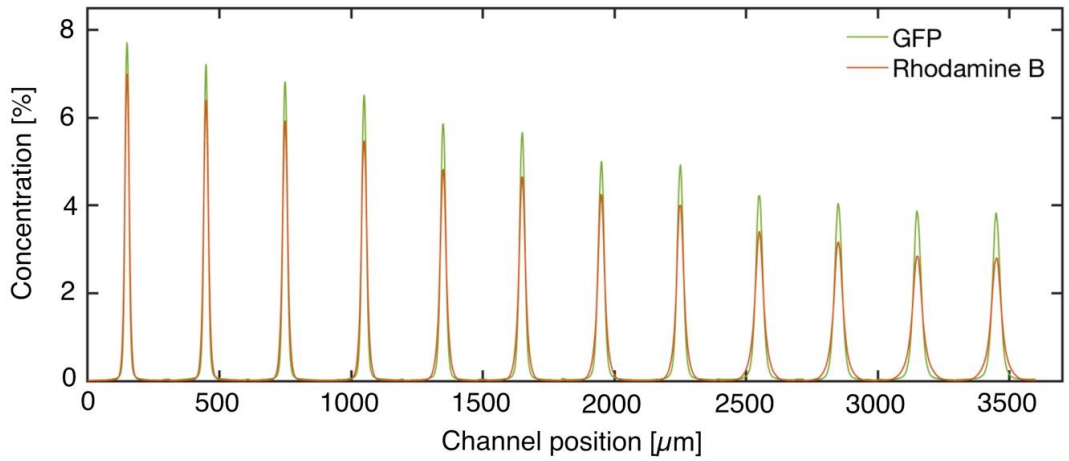

Figure S2. Diffusion profiles along the microfluidic channel of the mixture of rhodamine-containing LUV and SUV and GFP-containing LUVs. When only GFP was excited, the diffusion profile at the end of the microfluidic channel appeared narrower that the ones obtained for rhodamine, meaning that the GFP-containing particles are larger.

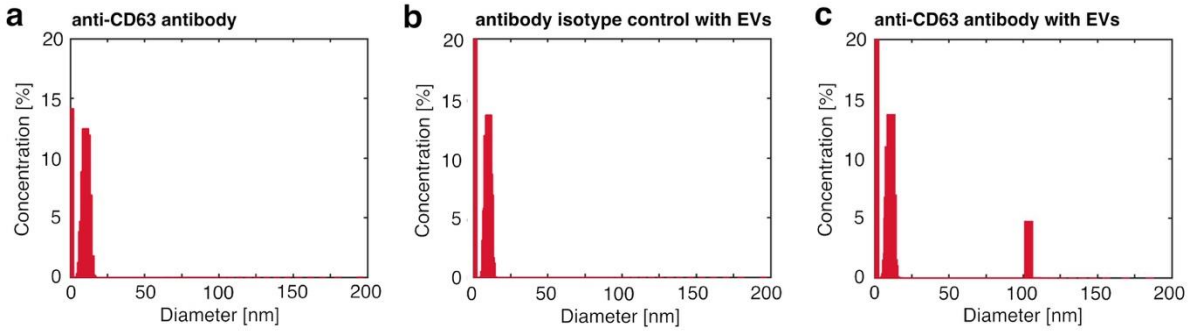

Figure S3. Binding specificity of the anti-CD63 antibody to CD63-positive EVs. (a) The anti-CD63 antibody alone did not form large aggregates. (b) Fluorescent particles were not detected when blocked EVs were mixed with an isotype of the anti-CD63 antibody. (c) In contrast, a peak corresponding to EVs was observed when the anti-CD63 antibody was added to EVs.

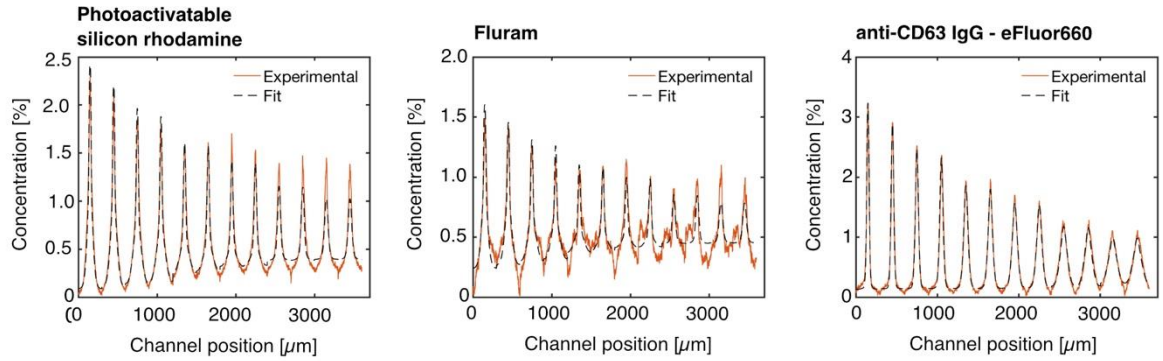

Figure S4. Experimental and fitted diffusion profiles obtained for the MSC-EV sample stained with a photoactivatable silicon rhodamine, Fluram and an anti-CD63 IgG coupled to eFluor660.

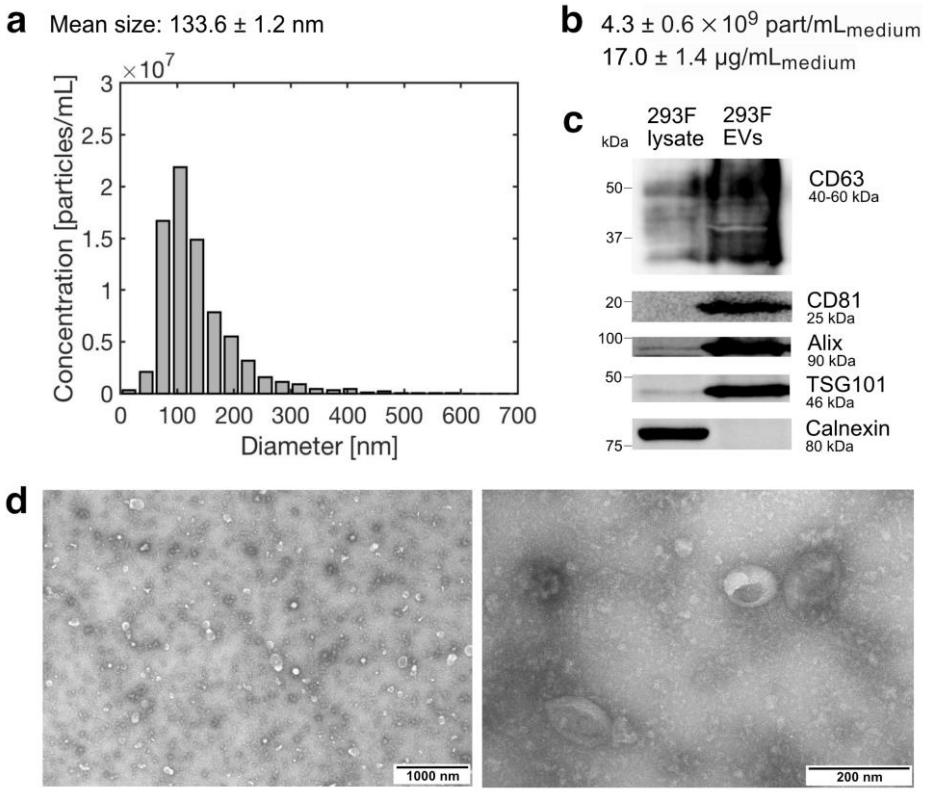

Figure S5. Characterization of 293F-derived EVs. (a) NTA in light scattering mode of particle size distribution. (b) Sample particle and protein concentration measured by NTA and μBCA, respectively. (c) Western blot for EV markers (CD63, CD81, ALIX, TSG101) and potential contaminant (Calnexin). (d) TEM pictures at 5000- and 35000-times magnification of the EV samples.

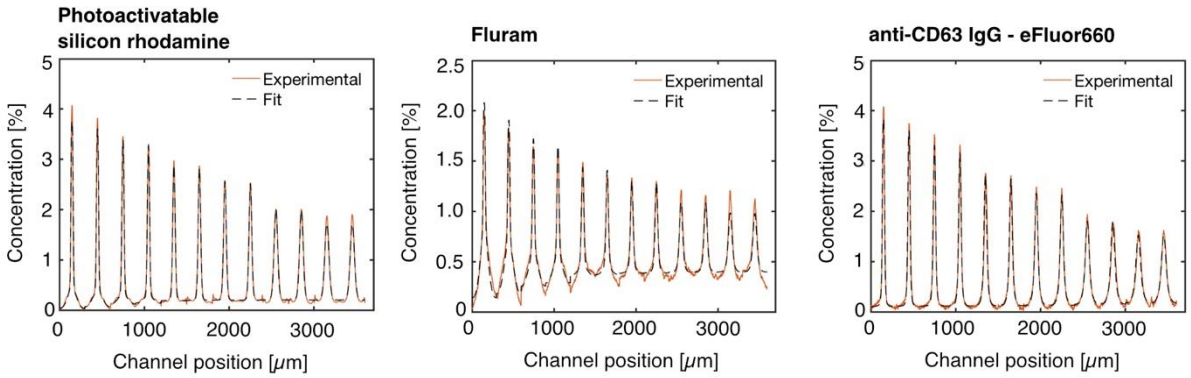

Figure S6. Experimental and fitted diffusion profiles obtained for the 293F-EV sample stained with a photoactivatable silicon rhodamine, Fluram and an anti-CD63 IgG coupled to eFluor660.